# Electronic structure of Ni and Pd alloys. III. Correlation effects in the Auger spectra of Ni alloys

Peter A. Bennett,* John C. Fuggle, and F. Ulrich Hillebrecht
*Institut für Festkörperforschung der Kernforschungsanlage Jülich, D-5170 Jülich, Federal Republic of Germany*
Albertus Lenselink and George A. Sawatzky
*Laboratory of Physical Chemistry, Materials Science Center, University of Groningen, 9747 Groningen, The Netherlands*
(Received 11 May 1982)

We have measured the Ni $L_3VV$ Auger spectra of 27 Ni alloys. The line shape, including multiplets, is calculated with the use of a method based on an approximate solution developed by Cini for a filled $s$ band. For Ni metal and its alloys, we have determined the values of $U^A$, the shift of the *main* Auger peak with respect to the energy calculated for Auger final states in which the two final-state holes are uncorrelated. We find changes in $U^A$ to be less than 1.4 eV, despite changes in Ni $d$-band occupation and in the density of states at the Fermi level. An "excitonic" screening mechanism which explains these features is discussed. The Ni $L_3VV$ feature sharpens considerably in alloys with, for instance, Al, La, and Th, so that the $d^8$ multiplet structure can be partially resolved. Two new mechanisms of line-shape broadening are found to dominate the Auger linewidths. The mechanisms are "hole-assisted dispersion," arising from the holes in the Ni $d$ bands, and "dissociational broadening," in which one of the valence-band holes left by the Auger process can move on to the partner-element site.

## I. INTRODUCTION

Parts I and II of this work, subsequently referred to as paper I (Ref. 1) and paper II,[2] dealt with x-ray photoelectron spectra (XPS) of the valence-band and core-level spectra of Ni and Pd alloys. While the effects of correlation between the valence electrons were important in those spectra, they did not dominate them. Here we consider the $L_3VV$ Auger spectra of Ni where the correlation effects are so pronounced that the spectra yield quantitative information on their strength.[3–12] Our purposes here are to present experimental data from Ni alloys, to treat some of the complexities involved in interpreting the data, and to discuss some implications of the results.

The modern view of $CVV$ Auger spectra basically dates from the recognition that the shape of these spectra was, in general, not given by simple self-folds of the one-particle densities of states.[13–19] $CVV$ Auger spectra result from nonradiative decay of a core hole $C$, with binding energy $E_B(C)$, to leave two holes in the valence band. We measure a quantity $U$ defined by

$$E_K(CVV)=E_B(C)-[E_B(V_1)+E_B(V_2)]-U\ , \tag{1}$$

where $E_B(V_1)$ and $E_B(V_2)$ are the binding energies of two independently created valence-band holes derived from XPS. In the simple Hubbard approximation[20] for narrow-band metals, $U$ can be identified with the "correlation" energy between two valence electrons and is a parameter of central importance in the theory of such materials. It is obvious that an accurate measurement of $U$ does not solve the correlation problem in narrow-band metals. Nevertheless a knowledge of the value of $U/W$, where $W$ is the bandwidth, does indicate whether a bandlike or atomlike starting point is more appropriate for discussing the properties of a metal or alloys.[21,22]

It is difficult to calculate $U$ for valence electrons even within the Hubbard approximation in which only intra-atomic correlations are considered since it is strongly reduced from its free-atom value by a variety of screening and relaxation processes.[21,23] This makes experimental values for $U$ of particular interest. By alloying, one can change the values of

 

the parameters which should affect the screening process, such as free-electron density, the position of the Fermi level, crystal structure, etc. The results of the present study of nickel and its alloys should be of interest both because we determine values for $U$ in the alloys, and because they should contribute to the understanding of screening in solids.

The shape of the Auger spectrum is also interesting since for large values of $U$ (as found in copper, for example) the two-hole final state is split off from the one-hole band states, and even shows the multiplet structure of the $3d^8$ atomic configuration.[3,18,24–28] In the case of Ni, where $U$ is approximately equal to the one-hole bandwidth, the two-hole states mix strongly with the band states. This mixing is of great importance to the magnetic and transport properties of the solid.[12,21–23] Another interesting problem in nickel is that the Fermi level is below the top of the $d$ bands. The two-hole problem including correlation effects is exactly soluble for filled bands, but only recently have attempts been made to treat the problem for unfilled bands.[9,29]

The $CVV$ Auger spectrum provides a good experimental testing ground for a study of the above problems. Nickel is particularly suitable for such studies since by alloying one can change the $U/W$ value through the interesting region between band-like and atomlike behavior, and change the band filling such that the number of ground-state holes becomes essentially zero. Also, Ni is perhaps more suitable than Pd and Ag systems since the $2p$ spin-orbit splitting clearly separates the $L_3VV$ from the $L_2VV$ spectra, and the $j$-term splitting within the $3d^8$ configuration is small.[30]

## II. BACKGROUND AND THEORY

In the $CVV$ Auger transition one valence electron fills an initial core hole and a second is emitted from the solid. The energy spectrum of the escaping Auger electron is given in the sudden approximation and neglecting matrix-element variations by the local two-hole spectral function $D(E)$ shifted by the binding energy (BE) of the core electron.[7,8] This is illustrated in Fig. 1.

For noninteracting holes, $D(E)$ is given simply by the self-fold of the local one-hole density of states, $n(E)$, shown as the dashed line in the figure. A repulsive interaction, $U$, of correlated holes lowers the kinetic energy (KE) of the Auger electron and, in general, changes the shape of $D(E)$. This moves the peak maximum away from the center of the self-fold by slightly more than the energy $U$.

Cini has derived an approximate solution for $D(E)$ for the case of a filled, nondegenerate band

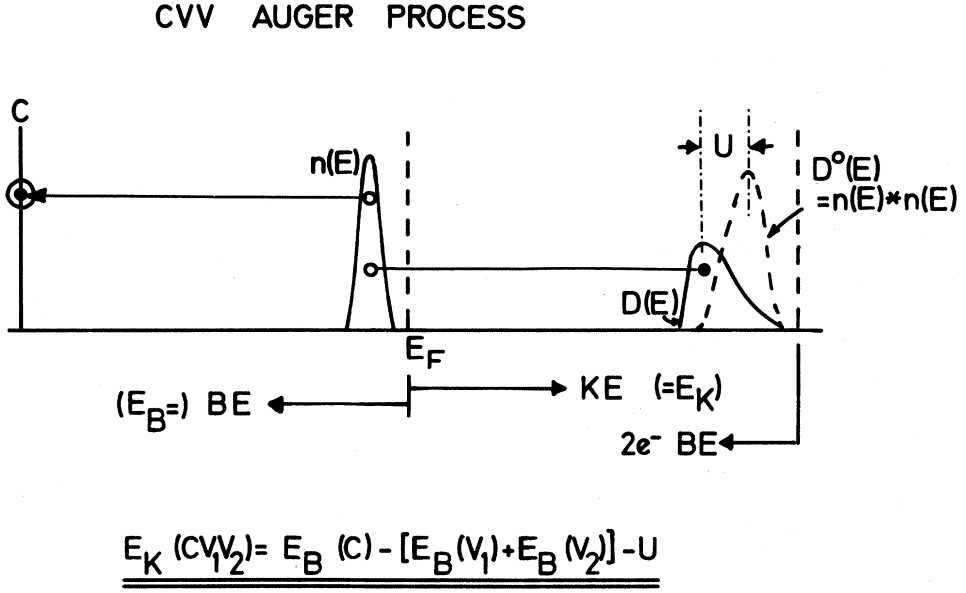


FIG. 1. Schematic diagram of the parameters involved in $CVV$ Auger processes. The diagram illustrates what is measured and how the measured kinetic energy is related to the correlation energy $U$. $n(E)$ represents the ground-state DOS, and $D^0(E)$ is the self-fold at $n(E)$ shifted by the core-hole binding energy. $D(E)$ represents the measured spectrum. Other details are given in the text.

which is as follows[5]:

$$D(E)=\frac{D^0(E)}{[1-UF(E)]^2+U^2D^0(E)^2}\ , \tag{2}$$

where $D^0(E)$ is the self-fold of the one-hole density of states $n(E)$,

$$D^0(E)=\int_0^{E_F} n(E')n(E-E')dE'\ , \tag{3}$$

and $F(E)$ is the Hilbert transform of $D^0(E)$ given by

$$F(E)=P\int_{-\infty}^{\infty}\frac{D^0(E')dE'}{(E-E')}\ . \tag{4}$$

While $D(E)$ can be determined by Auger spectroscopy, $D^0(E)$ is the density of two-hole states neglecting the electron-electron interaction and therefore cannot be directly determined from photoemission. For $D^0(E)$ one should use a self-convolution of the calculated one-particle density of states, but this is not feasible in many of the alloys studied here.

The resulting spectrum for a rectangular density of states (DOS) of width $W$ is sketched in Fig. 2 for several choices of $U/W$. As $U/W$ increases from zero the spectrum rapidly distorts from the self-fold of $n(E)$ (shown as a dashed line in the top panel) with a pronounced skewing to larger two-electron binding energy (lower kinetic energy of the Auger electron). For larger $U$ values ($U/W>1$) a true bound state appears, split off from the bandlike states which occupy the region of the self-convolution. Spectral weight is rapidly transferred to this split-off state for increasing $U$ values. The split-off state is sketched here with a finite width, although this is not included in Eq. (2). This results from dispersion of the excitonlike two-hole bound state, as described in the exact solution.[7]

The energy difference between the centroids of $D(E)$ and $D^0(E)$ is exactly $U$ for any $n(E)$ (as long as the bands are full), thereby providing a criterion for determining $U$. Since it is experimentally impractical to determine the centroid of the Auger spectrum, however, we define a $U^A$ measured from the peak maximum and will use it to infer a value for $U$. In Fig. 3, we show the ratio $U^A/W$ as a function of $U/W$ for several model DOS's, where $D(E)$ has been calculated using Eq. (2). For most of the nickel alloys, we find $U^A/W$ values larger than 0.85, so $U^A$ will typically exceed $U$ by 20% or less. Thus for our purposes we need not directly calculate Eq. (2) for each case.

A serious problem in the choice of $n(E)$, however, arises in the case of nickel since correlation effects between the photoemission and ground-state holes give rise to a satellite peak in the measured valence-band (VB) spectrum.[1,31–40] From an atomic viewpoint, the spectrum contains a mixture of "$3d^8$" and "$3d^9$" final states, the former comprising the satellite feature. A comparison with the *CVV* Auger spectrum shows that the valence-band satellite energy is the same as that of the Auger final state, which helps substantiate the above description.[1,39] For the problem at hand we need to determine the energy for a single $3d$ ionization, and at least the general effect of the ground-state holes on the Auger line shape.

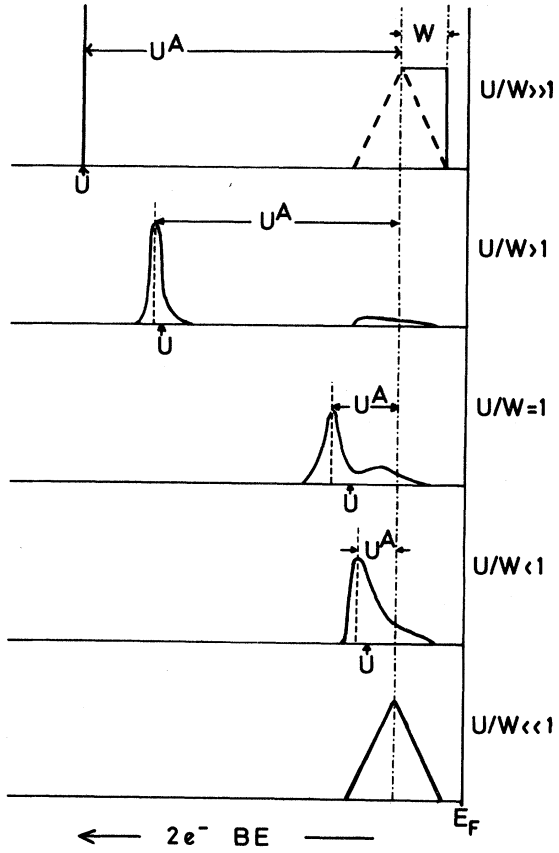


FIG. 2. *CVV* spectra calculated for a rectangular DOS of width $W$. Spectra have been calculated with the Cini approximation (Ref. 5) using several values of $U/W$.

Recently,[29,38] it has been proposed that the Auger spectrum for unfilled bands may be calculated by again using Eq. (2) but with substitution of $\tilde{D}^0(E)$ for $D^0(E)$, where

$$\tilde{D}^0(E)=\int_0^{E_F}\tilde{n}(E')\tilde{n}(E-E')d(E')\ , \tag{5}$$

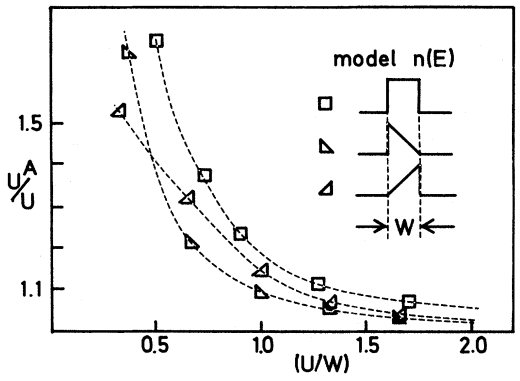


FIG. 3. Plots of $U^A/W$ as a function of $U/W$ for several model DOS's. $U^A$ is the "correlation" energy measured from the Auger peak, whereas $U$ is that measured from the Auger centroid.

i.e., the suggestion was to replace the one-electron DOS $[n(E)]$ by the spectral function $\tilde{n}(E)$. To test this we used for $\tilde{n}(E)$ our measured valence-band spectrum after subtraction of a background, but not the satellite. Figure 4 shows the result of doing this for Ni.

The two-hole spectral function $\tilde{D}(E)$ is calculated from Eq. (2) using a $U$ value of 2.5 eV. Also shown in the middle panel of Fig. 4 are the $\tilde{n}(E)$ and $\tilde{D}(E)$ calculated by Treglia *et al.*[9,41] with $W=4$ eV and $U=2.4$ eV and 0.6 holes/atom. The main differences between the two $\tilde{D}^0(E)$ in Fig. 4 arise from differences in the $\tilde{n}(E)$ used and show that the choice of $\tilde{n}(E)$ is important. The most important point to notice is that both calculations give the major $\tilde{D}(E)$ peak a $2e^-$ (BE) of $\sim 8$ eV. This is about 2 eV higher than the $d^8$ satellite found in photoemission or in the calculated $\tilde{n}(E)$, and is in direct contradiction to the experimental result where the $d^8$ energies found by XPS and $L_3VV$ Auger spectroscopy are identical in all alloys studied (see Table VI in paper I). We note that the $\sim 8$-eV peak in $D(E)$ arises from convolution of $\tilde{n}(E)$ when holes in the $d^8$ satellite and the $d^9$ band are combined. Its large weight is a result of the Hilbert transformation. In our opinion the 8-eV peak in $\tilde{D}(E)$ corresponds to $d^7$-like states.

Although the $\tilde{D}(E)$ curves in Fig. 4 bear superficial resemblance to the experimental curve, it is not possible to retain the resemblance and to line up the main peaks in $D(E)$ with the experimental Auger spectral peaks using Eq. (5). Adjustment of the $U$ values gives either a two-electron BE which is too large or a linewidth which is too broad. Inclusion of the multiplet structure would, of course, broaden

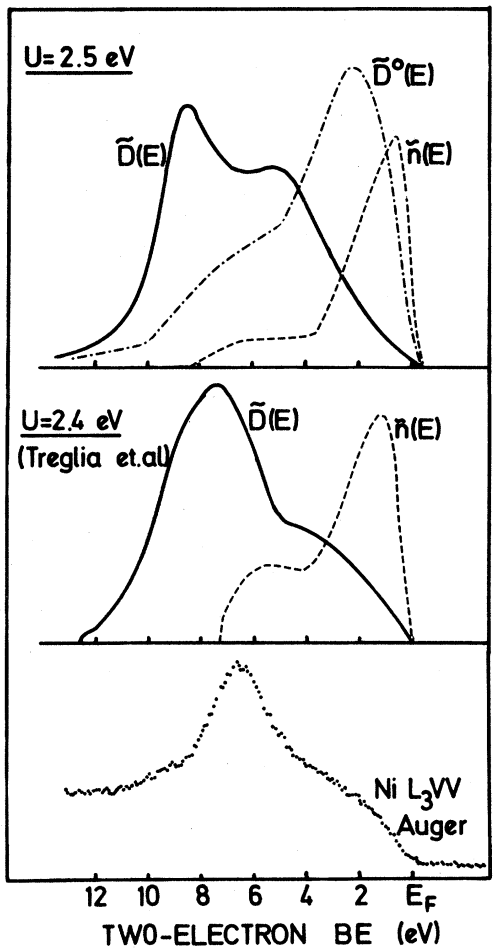


FIG. 4. Calculated Ni $L_3VV$ Auger spectrum of Ni [$\tilde{D}(E)$ is represented by ——] obtained from Cini formula [Eq. (2)] after substitution of the XPS spectrum, $\tilde{n}(E)$ (— — —) for the one-particle density in Eq. (3). $\tilde{D}^0(E)$ (—·—·—·) is the result of a self-fold of $\tilde{n}(E)$. The experimental Auger spectrum is also shown for comparison. No multiplet splitting is included in the calculation.

the line further.[41]

We suggest two reasons for the failure of this calculation to reproduce the experimental line shape. First, the final-state energies are not correct. In an atomic description, the self-fold $\tilde{D}^0(E)$ contains terms corresponding to $d^8$ and $d^7$ configurations, separated by approximately the one-electron $(d^9)$ BE. A $d^6$ term, also present, is off scale. The energy of a $d^7$ term, however, should be separated $2U^A$ from the $d^8$ term since there are *two* additional interaction energies for the three-hole cases. Because this term is so far away it should receive very little spectral weight. Second, the calculation ignores initial-state screening effects which would transfer

charge to the site of the Auger decay. The initial state with the core hole should then be predominantly $3d^{10}$ rather than $3d^9$. To first order this screening would have the effect of weighting the $d^8$ final state very strongly compared to the other terms.[7,8,42]

To proceed with our estimate of $U^A$ for the series of alloys we will simply truncate the satellite from the measured valence-band spectrum and use the centroid of the remaining spectrum to represent the energy of a "screened $d^9$" configuration, i.e., the single-ionization energy of the $3d$ shell. Inclusion of the satellite (using the spectrum shown in Fig. 4) would increase the BE of the centroid in pure nickel by 0.5 eV which in turn would reduce our value of $U^A$ by $\sim 1.0$ eV. This ambiguity in determination of the valence-band centroid is presumably smaller for alloys in which the satellite intensity is reduced compared to pure nickel.

Next we consider the multiplet structure of the spectrum. The extension of Eq. (2) to the case of degenerate bands has been outlined in Ref. 37 where it was pointed out that if the effective potential is predominantly spherical the terms in the $d^8$ configuration will not mix. The Auger spectrum then is the sum of independent terms whose shapes are given by Eq. (2) with an appropriate set of $U$ values. This procedure has been shown to work well for the cases of Zn, Ga, and Ge in which all terms of the $L_3VV$ spectrum are clearly split off from the band states.[3,43] We find favorable results (as follows) for the case of nickel, where $U/W < 1$ allowing considerable mixing of the two-hole and one-hole states.

From atomic theory, the energies of the five terms of the $d^8$ configuration are given as linear combinations of the Slater integrals $F^{(0)}$, $F^{(2)}$, and $F^{(4)}$.[44] The latter two determine the splitting between terms, while the $F^{(0)}$ term moves the configuration as a whole.[44] In the Ga $L_3VV$ spectrum we found that the $3d^8$-multiplet splittings remain nearly at their atomic value for atoms in the solid states while the $F^{(0)}$ term is strongly reduced due to screening and relaxation effects.[3] In the same work it was shown that experimental transition probabilities agree well with the calculated values, for example from McGuire.[45] We should note here that the transition probabilities for the $L_3M_{4,5}M_{4,5}$ transition are much larger than those for $L_3M_{4,5}N$ or $L_3N_1N_1$ transitions (i.e., $s$ final-state holes). The contribution to the line shape from such states would in any case be very broad and shifted to higher kinetic energy since the $4s$-$3d$ or $4s$-$4s$ Coulomb interaction is very small. Therefore we wish to use only the nickel $3d$ DOS for $n(E)$ in Eq. (3) and will compare $D(E)$ with the total $L_3VV$ spectrum.

We show examples of the expected multiplet structure in Fig. 5. For $n(E)$ we have used the experimental valence-band spectrum after truncation of the satellite feature and with the addition of a very small tail of intensity at higher BE which artificially broadens the split-off states.[46] This spectrum as well as the self-fold are shown in the lower panel. We have used Mann's calculated values of

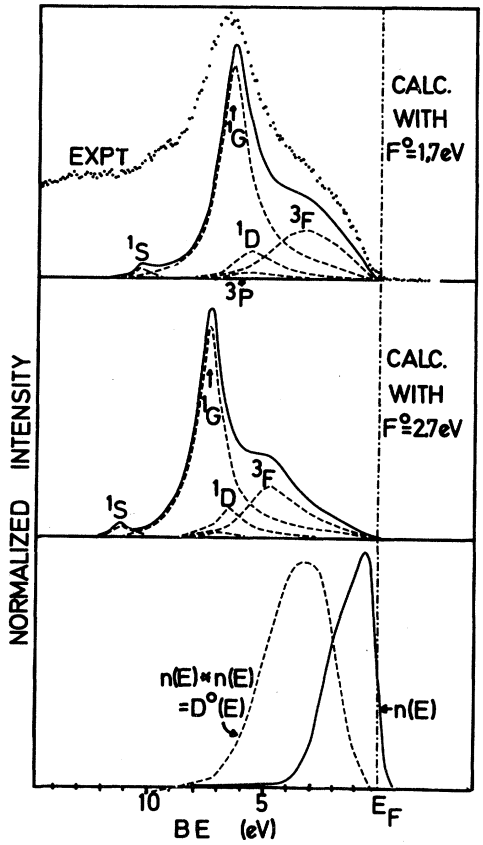


FIG. 5. Effect of multiplets on the Ni $L_3VV$ Auger spectra. Lower panel: XPS VB after subtraction of satellite $N(E)$ and its self-fold $D^0(E)$. Middle panel: calculated contributions to the Ni $L_3VV$ spectrum from the individual $d^8$ terms with slater integrals $F^{(0)}=2.7$ eV, $F^{(2)}=9.6$ eV, and $F^{(4)}=6.1$ eV, which gives $U(^1S)=7.3$ eV, $U(^1G)=3.5$ eV, $U(^3P)=2.85$ eV, $U(^1D)=1.6$ eV, and $U(^3F)=1.0$ eV. Top panel: calculated contributoins to the Ni $L_3VV$ Auger spectrum with $F^{(0)}=1.7$ eV, $F^{(2)}=9.6$ eV, and $F^{(4)}=6.4$ eV, which gives $U(^1S)=6.3$ eV, $U(^1G)=2.5$ eV, $U(^3P)=7.85$ eV, $U(^1D)=1.6$ eV, and $U(^3F)\approx 0$ eV. The experimental Auger spectrum is shown for comparison.

$F^{(2)}$ and $F^{(4)}$ (Ref. 47) for nickel $3d^8$ but have reduced it by 20% to allow for solid-state screening, while the $F^{(0)}$ value has been adjusted to bring the position of the $^1G$ term near to its experimental value.

The results are interesting because some terms like the $^1G$ or the $^1S$ are clearly split off from the band states while others like the $^3F$ are still within this region and can strongly mix with the band states. As the $F^{(0)}$ value is increased, the multiplet moves out of the region of band states, as illustrated in the top two panels of Fig. 5. Consequently, the terms of the multiplet narrow so that the $^3F$ term changes from a shoulder into a partially resolved peak. We find this sort of change in the experimental spectra of the alloys, as discussed in Sec. III. They have also been found for Pd and Ag alloys,[48,49] where narrowing of the valence bands in, for instance, Mg-Ag alloys leads to large increases of $U/W$ for the $M_{4,5}VV$ Auger spectra. We have

TABLE I. $L_3VV$ Auger-peak energies and related data (all values in eV).

| Material | Auger KE | $2p_{3/2}$ BE | $2e^-$ BE | VB centroid $E$ | $U^A(^1G)$[a] | $W$ | $U^A(^1G)/W$ |
|---|---|---|---|---|---|---|---|
| Ni | 846.2 | 852.65 | 6.45 | 1.40 | 3.65 | 3.8 | 0.95 |
| $MgNi_2$ | 845.80 | 852.85 | 7.05 | 1.40 | 4.25 | 3.3 | 1.30 |
| $Mg_2Ni$ | 845.80 | 852.7 | 6.90 | 1.35 | 4.2 | 2.7 | 1.55 |
| $AlNi_3$ | 845.80 | 852.65 | 6.85 | 1.50 | 3.85 | 4.0 | 0.95 |
| AlNi | 845.30 | 852.8 | 7.50 | 1.65 | 4.20 | 3.5 | 1.20 |
| $Al_3Ni_2$ | 844.80 | 853.4 | 8.60 | 2.15 | 4.30 | 2.85 | 1.50 |
| $Al_3Ni$ | 844.85 | 853.75 | 8.90 | 2.50 | 3.90 | 2.4 | 1.60 |
| ScNi | 845.95 | 852.8 | 6.85 | 1.60 | 3.65 | 3.2 | 1.1 |
| TiNi | 845.70 | 853.15 | 7.45 | 1.75 | 3.95 | 3.8 | 1.05 |
| $CrNi_2$ | 845.90 | 852.95 | 7.05 | 1.60 | 3.85 | 4.0 | 0.95 |
| CuNi | 846.25 | 852.55 | 6.30 | | Ni 3*d* VB obscured by Cu 3*d* | | |
| PdNi | 846.50 | 852.45 | 5.95 | | Ni 3*d* VB obscured by Pd 4*d* | | |
| InNi | 845.90 | 852.35 | 6.45 | 1.35 | 3.75 | 3.05 | 1.25 |
| $LaNi_5$ | 846.15 | 852.6[b] | 6.45 | 1.50 | 3.45 | 3.7 | 0.9 |
| LaNi | 845.80 | 852.9[b] | 7.10 | 1.65 | 3.8 | 3.0 | 1.25 |
| $La_7Ni_3$ | 846.20 | 852.75[b] | 6.55 | 1.75 | 3.05 | 2.1 | 1.45 |
| $La_3Ni$ | 846.00 | 852.7[b] | 6.70 | 1.90 | 2.90 | 2.1 | 1.40 |
| $CeNi_5$ | 846.15 | 852.6 | 6.45 | 1.35 | 3.75 | 3.7 | 1.00 |
| $CeNi_2$ | 846.00 | 853.00 | 7.00 | 1.65 | 3.70 | 3.6 | 1.05 |
| CeNi | 846.0 | 853.00 | 7.00 | 1.70 | 3.6 | 2.8 | 1.30 |
| $Ce_7Ni_3$ | 845.90 | 853.00 | 7.10 | 1.90 | 3.3 | 2.4 | 1.40 |
| $TaNi_3$ | 845.90 | 852.75 | 6.85 | 1.40 | 4.05 | 4.2 | 0.95 |
| $TaNi_2$[c] | 845.65 | 853.20 | 7.55 | 2.0[c] | 3.55[c] | 4.1[c] | 0.85[c] |
| $Ta_2Ni$[c] | 845.7 | 853.3 | 7.6 | 2.10[c] | 3.2[c] | 4.2[c] | 0.75[c] |
| AuNi | 847.85 | 852.15 | 5.30 | ~1.10 | ~3.10 | | |
| $ThNi_5$ | | | | 1.40 | | 3.7 | |
| ThNi | 845.80 | 853.0 | 7.20 | 1.85 | 3.5 | 3.0 | 1.20 |
| $Th_7Ni_3$ | 845.95 | 853.15 | 7.20 | 2.0 | 3.2 | 2.6 | 1.25 |
| Cu | 918.8 | 932.35 | 13.55 | 3.30 | 7.10 | 4.1 | |
| $MgCu_2$ | 918.7 | 933.1 | 14.4 | 3.30 | 7.80 | 3.3 | |
| $Mg_2Cu$ | 918.6 | 933.4 | 14.8 | 3.90 | 7.00 | 2.3 | |
| NiCu | 918.25 | 932.45 | 14.2 | 3.50 | 7.2 | ~4 | |

[a]There may be a small systematic error in $U^A$ due to uncertainty in subtraction of the VB satellite.
[b]$2p_{1/2} - 17.2$ eV.
[c]Full width at half maximum (FWHM) and centroid probably influenced by Ta levels.

not attempted an exact fitting to the experimental line shape since in most of the alloys only one term in the configuration can be experimentally resolved. Further, the calculated shape of a single term is not well known when its $U$ value approaches the split-off condition ($U/W>1$) since here the dispersion of the two-hole state which is not included in Eq. (2) may become significant[7,8] and the shape given by Eq. (2) is very sensitive to structure in $n(E)$ near the bottom of the band.

We make two points, however, regarding the multiplet structure: Firstly, the $^1G$ term clearly dominates the spectrum, contributing $\sim\frac{2}{3}$ of the integrated intensity. This is the term whose $U^A$ we list later in Table I. Since its energy is given by

$$U(^1G)=F^{(0)}+\tfrac{4}{49}F^{(2)}+\tfrac{1}{441}F^{(4)}$$

(Ref. 44), its position is not too sensitive to uncertainty in the choice of the $F^{(2)}$ and $F^{(4)}$ values. Secondly, the width of the peak near its maximum can be fairly accurately interpreted to arise from a *single* term, this being the $^1G$. Any possible overlap of multiplets would contribute an asymmetric broadening of the peak to higher kinetic energy, which should be experimentally apparent.

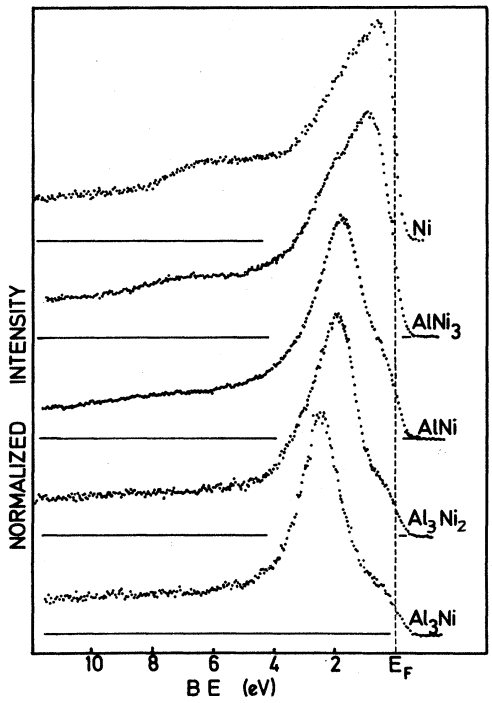


FIG. 6. XPS spectra of the VB's of Al-Ni alloys showing the narrowing of the Ni $d$ bands as the Ni content decreases. This is a typical result for alloys with electropositive metals.

## III. EXPERIMENTAL RESULTS

Details concerning sample preparation and the apparatus are given in papers I and II. Auger spectra presented here were excited with Al$K\alpha$ radiation except when an overlap Auger and XPS peaks made use of Mg$K\alpha$ radiation more appropriate. We presented the valence-band and core-level spectra of all the nickel and palladium compounds we have studied in papers I and II. Here we illustrate the behavior of the valence-band spectra with the example of the aluminium-nickel compounds shown in Fig. 6. We find that with increasing dilution of nickel with more electropositive partner metals, the nickel $3d$ bands become narrower and pull away from the Fermi level. Concurrent with this, the satellite feature essentially disappears. At the excitation energy of $h\nu=1486.7$ eV photoemission from the nickel $d$ bands dominates the spectrum, although some contribution from aluminium and nickel $sp$ states is also present.

In the appendix to paper I we described the methods of background subtraction used for the valence bands of Ni alloys. We always subtracted the satellite contribution, if one was present, and decided that the uncertainties in definition of the Ni $d$-band centroids and effective widths were approximately 0.3 eV. Inclusion of the satellite feature would increase the centroid BE of the Ni spectrum by $\sim 0.5$ eV.

The Auger spectra are shown in Figs. 7–11. No background correction has been made, so that a considerable amount of intensity is present at lower kinetic energies due to inelastic scattering of the escaping electron. The peak maxima have been aligned and the intensity normalized to show more clearly the changes in line shape. The $U$ values appropriate to these spectra are given in Table I.

We show our values for $U^A$ in Table I along with the pertinent numbers used to determine it. The first two columns list the kinetic energies of the Auger-peak maxima and the $2p_{3/2}$ core-line BE's both given with respect to the Fermi level. The next column is the $3d$ double-ionization energy, which is simply column 2 minus column 1. We assign here an uncertainty of $\sim 0.3$ eV due mostly to the machine calibration and determination of the Fermi level. The next column gives the centroid of the nickel $3d$ states after removal of background and satellite contributions as previously described.

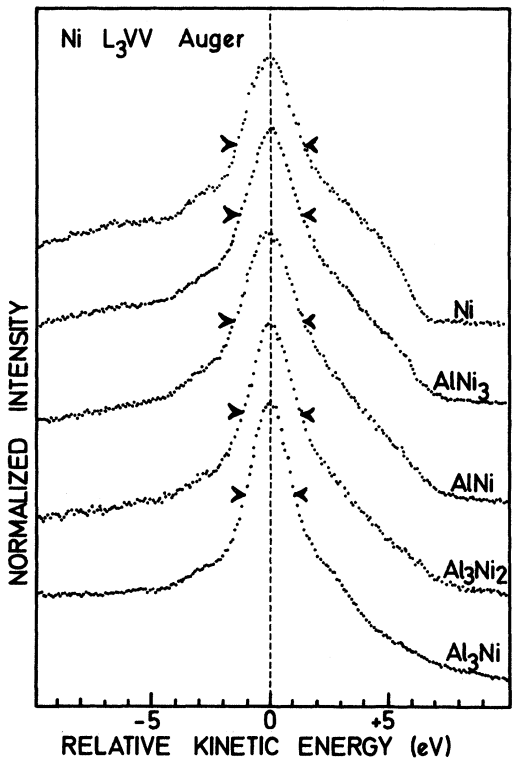


FIG. 7. X-ray-excited Ni $L_3VV$ Auger spectra from Al-Ni alloys. Spectra have been shifted to align the peak maxima and have been approximately normalized to give the same peak heights. Arrows indicating the full width at $\frac{2}{3}$ maximum intensity (measured with respect to the base line on the high-KE side) are shown to help compare the widths.

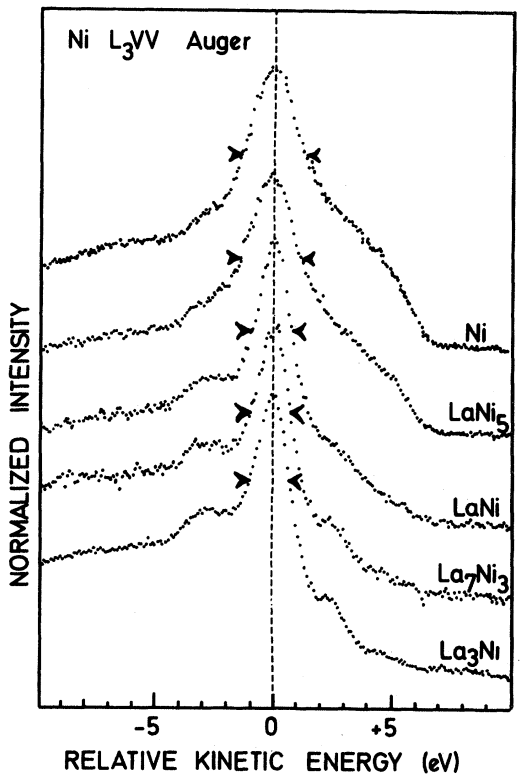


FIG. 8. Ni $L_3VV$ Auger spectra of La-Ni alloys. Other details as for Fig. 7.

The $U^A(^1G)$ values in the next column are simply column 3 minus twice column 4, and an overall uncertainty of 0.5 eV is assigned. The next column gives $W$, the effective width of the nickel $3d$ bands, determined as the base of a trapezoidal extrapolation of the measured spectrum. Details of this determination are given in paper I. The ratio $U^A(^1G)/W$ is given in the last column. At the bottom of the table are shown entries for the respective quantities for copper in a few copper alloys. The results for $U^A$ are fairly constant at $3.6\pm0.7$ eV for all the Ni alloys and $7.4\pm0.4$ eV for the Cu alloys measured.

Our characterization of the Auger linewidths is shown in Table II. The Auger linewidth is given in column 2. The precision in this number is 0.10 eV, limited mostly by the counting statistics. Typically $10^4$ counts at the peak maximum were accumulated. Because the different multiplet terms overlap and because of the large contribution from inelastically scattered electrons we have no ideal way to characterize the widths of the Auger peaks by a single number. We have used the full width of the Auger peak at $\frac{2}{3}$ maximum as this is at least a consistent procedure for detecting *trends* in line shape. At this height the width is dominated by the contribution from the $^1G$ term in the multiplet term. We argue that by measuring at the upper third of the peak we minimize the effects of the inelastic background as well as any smooth contribution from underlying multiplet terms. The nearly symmetric appearance of the line substantiates our procedure. The second column in Table II gives the measured full width at half maximum (FWHM) of the $L_3$ core level. This is intended as an estimate of three sources of broadening in the Auger line: instrumental broadening (0.4 eV FWHM in Auger, 0.6 eV in XPS), the $L_3$ lifetime width, and a low-energy tail due to Fermi-surface shakeup.[50] The latter contribution has been shown to be present in the $KL_2L_3$ Auger spectra of Na and Mg, and to produce an asymmetry parameter nearly equal to that of the

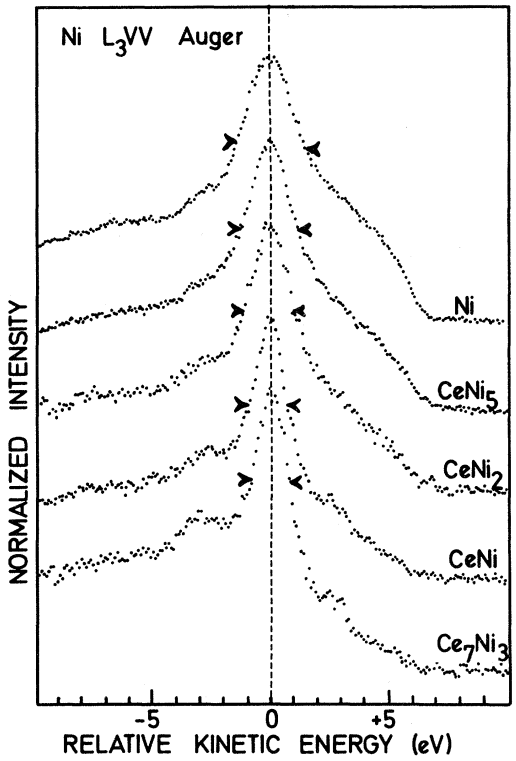


FIG. 9. Ni$L_3VV$ Auger spectra of Ce-Ni alloys. Other details as for Fig. 7.

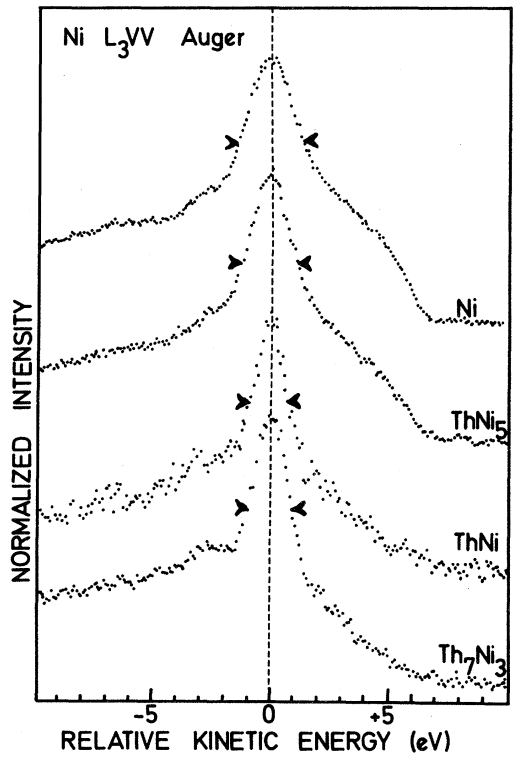


FIG. 10. Ni$L_3VV$ Auger spectra of Th-Ni alloys. Other details as for Fig. 7.

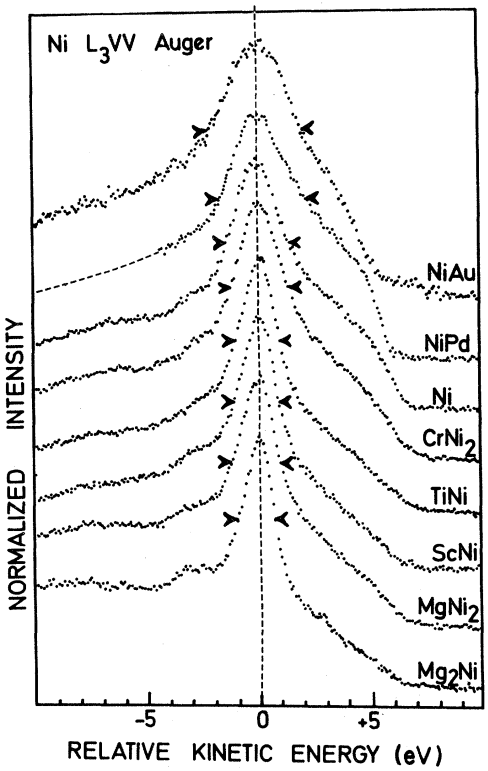


FIG. 11. Ni$L_3VV$ Auger spectra of $Mg_2Ni$, $MgNi_2$, $CrNi_2$, and some 1:1 alloys showing the variation in Auger linewidth. Other details as for Fig. 7.

XPS core lines.[51]

The third column of Table II, labeled "excess" width, is the difference of the first two. It gives a measure of that part of the Auger linewidths arising from two-hole dispersion, etc., as discussed in Sec. IV. The observation that this is almost zero in the copper alloys justifies, to some extent, our use of the full width at $\frac{2}{3}$ maximum ($W_{2/3}$) to characterize the width of the $^1G$ term.

Observing the changes in line shape for the aluminium-nickel series shown in Fig. 7 one sees that with increasing dilution of nickel the $^1G$ term narrows, and the pronounced bulge to higher kinetic energy in the pure-nickel spectrum changes to a concave shape. These changes we will correlate with other parameters in Tables I and II. This trend is also visible in the other series of compounds, being in fact more pronounced for electropositive partner metals. The lanthanum-nickel spectra in Fig. 8 are good examples. Here, the changes are large enough that the bulge at several eV above the peak maximum can be seen to evolve into a partially resolved peak. The resemblance to the calculated spectra of Fig. 5 is very good, and al-

TABLE II. Factors for the Ni $L_3VV$ $^1G$ Auger linewidths. (All values in eV; see text for details of width measurements.)

| Material | $L_3VV$[a] "width" | $L_3$ FWHM | "Excess" | Ni-Ni coordination number |
|---|---|---|---|---|
| Ni | 3.00 | 1.35 | 1.65 | 12 |
| $MgNi_2$ | 2.3 | 1.25 | 1.05 | 4 |
| $Mg_2Ni$ | 1.75 | 1.15 | 0.60 | 2 |
| $AlNi_3$ | 3.0 | 1.25 | 1.75 | 8 |
| AlNi | 3.0 | 1.25 | 1.75 | 6 |
| $Al_3Ni_2$ | 2.7 | 1.15 | 1.55 | 3 |
| $Al_3Ni$ | 2.15 | 1.10 | 1.05 | 0 |
| ScNi | 2.10 | 1.15 | 0.95 | 6 |
| TiNi | 2.15 | 1.20 | 0.95 | 6 |
| $CrNi_2$ | 2.55 | 1.4 | 1.15 | ? |
| CuNi | 4.0 | 1.30 | 2.70[b] | ~6 |
| PdNi | 4.0 | 1.45 | 2.55 | ~6 |
| InNi | 2.15 | 1.10 | 1.15 | 4 |
| $LaNi_5$ | 2.5 | 1.25 | 1.25 | ~8 |
| LaNi | 1.70 | (1.05)[c] | (0.65)[c] | 2 |
| $La_7Ni_3$ | 1.65 | (1.1)[c] | (0.55)[c] | 0 |
| $La_3Ni$ | 1.60 | [c] | | 0 |
| $CeNi_5$ | 2.45 | 1.25 | 1.2 | 8 |
| $CeNi_2$ | 2.30 | 1.15 | 1.15 | 6 |
| CeNi | 1.75 | 1.05 | 0.70 | 2 |
| $Ce_7Ni_3$ | 1.65 | 1.10 | 0.45 | 0 |
| $TaNi_3$ | 2.90 | 1.35 | 1.6 | 8 |
| $TaNi_2$ | 2.55 | 1.35 | 1.2 | 5 |
| $Ta_2Ni$ | 2.35 | 1.5 | 0.85 | 2 |
| AuNi | 4.10 | 1.40 | 2.70 | ~6 |
| $ThNi_5$ | 2.30 | 1.30 | 1.00 | ~8 |
| ThNi | 1.75 | 1.05 | 0.70 | ~1 |
| $Th_7Ni_3$ | 1.80 | 1.2 | 0.60 | 0 |
| Cu | 1.20 | 1.10 | 0.10 | |
| $MgCu_2$ | 1.20 | 1.10 | 0.10 | |
| $Mg_2Cu$ | 1.20 | 1.10 | 0.10 | |
| NiCu | 1.20 | 1.10 | 0.10 | |

[a]Peak full width at $\frac{2}{3}$ maximum ($W_{2/3}$).

[b]Overlap of Ni $L_3VV$ and Cu $L_3M_{2,3}M_{4,5}$.

[c]Ni $2p_{3/2}$ and La $3d_{3/2}$ XPS peaks overlap so Ni $2p_{3/2}$ widths are taken from the corresponding Ce compounds, where possible.

lows indentification of this feature as the $^3F$ term of the $3d^8$ configuration.

In the $La_3Ni$ spectrum, this peak is separated from the $^1G$ term by ~2.5 eV. This is close to the value of 2.65 eV found in the optical spectra of free Ni atoms,[30] which in turn is 20% smaller than that obtained from evaluation of the two-electron Slater integrals (3.1 eV).[47] The latter reduction is due principally to contraction of the $d$ orbital upon removal of two electrons. The further reduction in the splitting observed in the Auger spectrum is accounted for by the different $U^A/U$ values for the two terms. That is, the peak maximum is pulled further from its centroid for the $^3F$ compared to the $^1G$ term, bringing them closer together. Correcting for this effect in the spirit of the analysis in Fig. 3, we can infer a $U(^3F)$ value from the $^3F$ Auger final-state energy of ~0.4 eV.

Another interesting feature in the spectra appears at 3 eV kinetic energy below the $^1G$ term. From the multiplet calculation one expects to find a contribution from the $^1S$ term in this region of the spectrum with ~2% of the integrated intensity. However, it is known that a "vacancy satellite" structure also

occurs in this region as a result of a Coster-Kronig decay of an $L_2$ hole preceding the $L_3MM$ transition.[15,52] We presume that the $^1S$ term is not distinguishable from this vacancy satellite structure in the spectrum. It is interesting to note that this structure corresponds to a $d^7$ final state. Earlier we stated that a $d^7$ final state should be displaced from the $d^8$ by $\sim 2U^A$, yet it appears here (more easily seen in the Cu spectrum in Fig. 12) to be much closer than $2U^A$ ($\sim 14$ eV in Cu) to the $d^8$ states. This is because the initial state for the vacancy satellite is a $2p_{3/2}$ $(3d^9)$ configuration and is shifted by the XPS core-level satellite energy ($\sim 6$ eV) from a $2p_{3/2}$ $(3d^{10})$.

## IV. DISCUSSION

We first discuss the dependence of $U^A$ on chemical environment. Here it is appropriate to consider more carefully the quantity measured. We measure

$$U^A=[E(3d^8)-E_F]-2(\bar{C}-E_F)\,, \tag{6}$$

where $\bar{C}$ is the centroid of the measured valence band without the satellite. Apart from small corrections for $U^A/U$ discussed in Sec. II, the energy we measure is thus the energy required to localize two holes from bandlike Ni $d$ states onto a single atomic site.

In the Hubbard model, the Hamiltonian of a system is separated into a sum of single-particle and many-body interaction terms. The former give rise to the familiar one-electron band structure while the latter define the correlation energy $U^H$, and give rise to the intra-atomic Coulomb interaction energy. In his third paper[20] Hubbard illustrated his model with a half-filled $s$ band where $U^H$ was the energy required to localize two electrons on one atom. In that case, where each atom had one $s$ electron,

$$U^H=\Delta^+ +\Delta^-\,, \tag{7}$$

where $\Delta^-$ is the ionization energy and $\Delta^+$ is the electron affinity of an atom in a solid. It is not possible to give such a simple picture in Ni, with 9.4 electrons in its $d$ bands. Nevertheless if we remember that Hubbard's $U$ is the screened intra-atomic Coulomb correlation energy then it is clearly very closely related to the energy required to localize two holes in a single atomic site, as measured by us. Note, however, that we have adopted the convention of defining a separate $U^A$ for each atomic $d^8$ configuration.

Some confidence in our procedure to determine $U$ comes from the favorable comparison of our value with that found by calculating the photoemission spectrum of pure nickel.[34–38] A recent calculation including higher-order correlation effects proposed a value of $U=2.5$ eV.[35] Since this was done for a nondegenerate band, we should compare to our value of $U^A$ for the $^1G$ term alone, which is 3.65 eV.[53] The difference is partly accounted for by the ratio $U^A/U$, which from Fig. 3 is $\sim 1.2$ if we assume a square DOS and a one-electron bandwidth of 4.3 eV. Even if the agreement is not exact, the *variation* of $U$ with chemical environment should parallel that of $U^A$. As shown in Table I we find $U^A(^1G)$ values in the range of 3.0 to 4.3 eV. The correction for the ratio $U^A/U$ is minor ($\lesssim 15\%$) in all cases since $U^A/W \gtrsim 0.85$.

Before proceeding to discussion of the values and variation of $U^A(^1G)$ it is sensible to consider the effect of $F^{(2)}$ and $F^{(4)}$ and the role of other $d^8$ terms. Many of the alloys studied have sharper $L_3VV$ Auger spectra than Ni itself, so that a shoulder at low two-electron BE can be more clearly resolved. In Fig. 12, we show the spectra of Ni, $La_3Ni$, and Cu to illustrate the monotonic development of the spectra. In Cu there is a peak on the low two-electron BE side of the $^1G$ feature which can be clearly attributed to the $^3F$ term.[25] (Peaks on the high-BE side are attributed to double-ionization processes.[3,15,28]) The partially resolved peak in $La_3Ni$ is thus also attributed to the $^3F$ term.

A fit of the calculated Ni $L_3VV$ Auger-peak shape to the experiment in order to determine $F^{(2)}$ and $F^{(4)}$ is not feasible here. Such a fit would require extensive research into the energy-loss processes which cause much of the background of the low-KE side of the peaks, or use of coincidence spectra where the loss processes are suppressed.[52] It must also take into account the broadening processes discussed later. Nevertheless, calculations are useful to check that our assumptions are reasonable. For the calculations we used $F^{(2)}$ and $F^{(4)}$ values reduced by 20% from Mann's atomic values and $F^{(0)}$ adjusted to bring the $^1G$ term into agreement with experiment. With the use of observed XPS VB's of Ni and $La_3Ni$ the total calculated $L_3VV$ Auger spectra, shown as a full line in Fig. 12, strongly resemble the experiment. As discussed in Sec. II, it is the contribution of the $^3F$ term which is most strongly affected by changes in $U/W$. We have discussed in more detail elsewhere the implications of the low $U^A$ values associated with the $d^8(^3F)$ configuration.[12] Because of the $d^8$-multiplet splitting, the $^3F$ configuration clearly has an energy suffi-

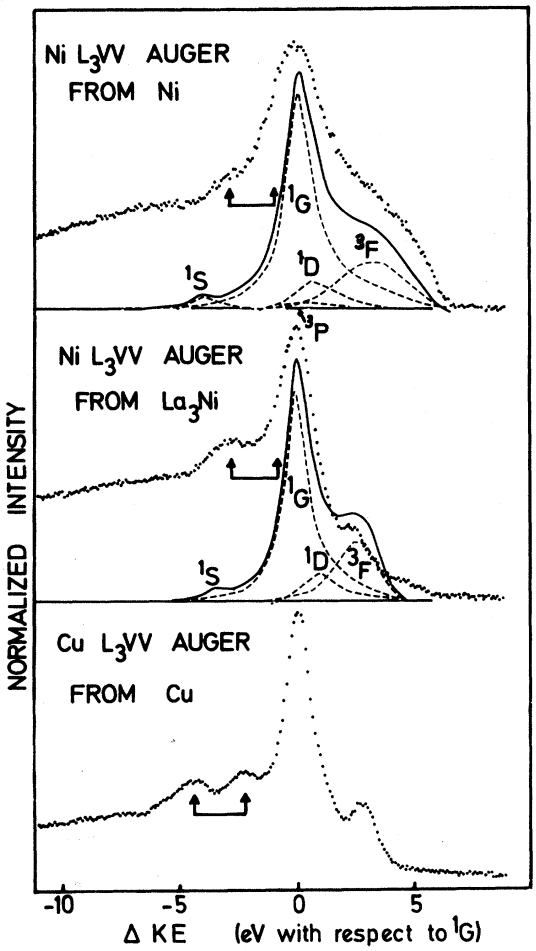


FIG. 12. Comparison of the Ni $L_3VV$ Auger spectra from Ni and $La_3Ni$ with the Cu $L_3VV$ spectrum of Cu. Also shown are the calculated total Ni $L_3VV$ Auger spectra and calculated contributions of the $^1G$ and $^3F$ terms. Parameters used for the calculation for Ni are $F^{(0)}=2.5$, $F^{(2)}=9.6$, and $F^{(4)}=6.4$; and for $La_3Ni$, $F^{(0)}=2.0$, $F^{(2)}=9.6$, and $F^{(4)}=6.4$ (all values in eV). These values correspond to $U(^1G)\sim 3.3, U(^3F)\sim 0.8$ for Ni and $U(^1G)\sim 2.7, U(^3F)\sim 0.4$ for $La_3Ni$.

ciently low to contribute to polar fluctuations in the ground state in Ni and Ni alloys. Although the importance of term splittings was recognized by Herring,[21] they have mostly been ignored in band-structure calculations since then because no direct experimental confirmation for the solid has been available. Because of the magnetic nature of the $^3F$ state its mixing into the ground state could be a determining factor in the description of the magnetic properties of Ni.[12]

Our conclusion that we have observed the $3d^8(^3F)$ term in alloys like $La_3Ni$ is supported by very recent synchrotron photoemission data from Ni where emission due to the $^3F$ term was found to increase in the Fano resonance at the $3p$ threshold. Within experimental uncertainty due to overlap of the $3d^8(^3F)$ term with the one-particle spectrum in Ref. 54, our results are in agreement for the $^1G$ and $^3F$ splitting in Ni. It is not possible to use the separation of the $^1G$ and $^3F$ terms found here to deduce accurate values for the Slater integrals $F^{(2)}$ and $F^{(4)}$. This is partly due to limited experimental accuracy, but also to the differences in the ratio of $U^A/U_{\text{eff}}$ for different values of $U^A/W$, as discussed in connection with Fig. 3. The $^1G$ term is outside the band and feels a different part of the real self-energy to the $^3F$ term inside the band.

However, we can conclude from comparisons such as those in Fig. 12 that the values of the Slater integrals $F^{(2)}$ and $F^{(4)}$ are nearly independent of the solid-state environment of the nickel atom in metallic compounds. This allows us to say that $U^A$ for the $^3F$ term is small and the $^3F$ term must be degenerate with the one-electron states in Ni itself and many of its alloys.

Knowing approximate values of $F^{(2)}$ and $F^{(4)}$ (see Fig. 12) we can infer an $F^{(0)}$ value from a measurement of $U(^1G)$ since

$$U(^1G)=F^0+\tfrac{4}{49}F^{(2)}+\tfrac{1}{441}F^{(4)}\,.$$

This gives $F^{(0)}$ values in the range of 2.4—3.7 eV for the entire alloy series.

It is common in discussions of relaxation and screening to separate "atomic" and "extra-atomic" contributions.[25,26,55,56] The atomic contribution is defined by calculating the relaxation energy for an isolated ion, and the rest is attributed to extra-atomic processes. In the present case, the relaxation energy is the reduction of the $F^{(n)}$ terms from their calculated free-atom values. Constancy of $F^{(2)}$ and $F^{(4)}$ means that the screening charge is spherically symmetric or that the monopole term in the many-body response is dominant.[57] The major effect of the relaxation is to change the $F^{(0)}$ term from $\sim 25$ to $\sim 3$ eV. In the sense described above we would assign $\sim 13$ eV to atomic relaxation since $U(^1G)$ evaluated for nickel atoms is $\sim 12$ eV.[20] The remaining 9 eV must be made up by extra-atomic relaxation or screening. This analysis leads one to expect a large variation of the relaxation energy with changes in chemical environment. In addition, the considerably smaller extra-atomic relaxation energy for the $L_3M_{4,5}M_{4,5}$ Auger line in copper compared to nickel has been attributed to a filling of the $d$ bands and consequent loss of $d$-electron screening[26,28]; however, see also Ref. 58. One might ex-

pect a similar effect in those alloys where the $d$ bands are essentially filled.

Contrary to the above arguments, we find that $U$ (and thus the relaxation energy) remains essentially constant upon alloying despite large changes in the free-electron density and the DOS near the Fermi level. We believe this is evidence for an excitonlike screening process[55,56] involving localized $4sp$ orbitals. In this sense, we would write the Auger final state in nickel and its alloys as $3d^8[4s^2]$, where the square brackets denote an occupied screening orbital which has been pulled below $E_F$ and localized by the $+2e$ charge of the $3d^8$ configuration. From our experiments we infer that the shape of the screening orbitals and thus the relaxation energy gained by their occupation is essentially independent of the chemical environment. On the same basis, the Auger final state in copper would be written $3d^8 4s^1[4s\,4p]^2$. In this case, screening the $+2e$ charge requires filling a $4p$ orbital as well as a $4s$ orbital. We would attribute the smaller relaxation energy in copper to a poorer screening by the $4p$ orbital compared to the $4s$ orbital. This may be due to the higher energy of the $4p$-band states.

The lack of any substantial variation of the relaxation energy with the density of $d$ states near the Fermi level may result from the following two considerations: Firstly, regardless of the quantity of unoccupied Ni $d$ states, or of unoccupied Ni $d$ character of other occupied bands in the initial state of Ni or its alloys, screening of the $2p_{3/2}$ core hole gives a local $d^{10}$ configuration in the Auger initial state. Secondly, the $d^8$ configuration resulting from Auger decay of the $2p_{3/2}$ core hole cannot be screened by transfer of a $d$ electron to the charged site since this would have a $d^9$ configuration. Such a transfer can, of course, occur, but this gives rise to the bandlike portion of the spectrum.

Next we consider the line shape. The first point to notice is that the $^1G$ term is split off from the Ni $d$ bands in essentially all cases, since $U/W \gtrsim 1$, which places the $^1G$ term below the bottom of the self-fold of $n(E)$. The exact criterion for a split-off state depends on details of the band structure, but our $U$ values are larger than the critical $U$ calculated for several model band structures,[8] particularly so since our measured $W$ must overestimate the true bandwidth. In this case, Eq. (2) predicts a $\delta$-function resonance. The exact solution of the problem, however, including the motion of the two-hole bound state through the lattice predicts a dispersion width of $\sim 0.5W(W/U)$.[7,8] Therefore, we expect this contribution to the linewidth to be $\lesssim 0.5$ eV. Recall that the entries in Table II labeled excess width have had the measured $L_3$ linewidth subtracted in an attempt to remove broadening due to instrumental resolution, the $L_3$ lifetime and the Fermi-surface shakeup. The small values listed for the excess linewidth in the copper alloys substantiate this procedure. Small increases in the width of the $^1G$ peak are expected as $U^A(^1G)/W$ is decreased. However, these effects are calculated to be smaller than $\sim 0.3$ eV in the range of $U^A(^1G)/W$ indicated in Table I and also fail to explain the observed effects. We must look for other mechanisms to explain the excess linewidths of 0.6 to 2.7 eV found in the nickel alloys. The mechanisms we envisage are illustrated schematically in Fig. 13.

The first process in Fig. 13(a) is the one we have labeled hole-assisted dispersion. We expect the propagation of the two-hole bound state through the lattice to be greatly enhanced for unfilled Ni $d$ bands as compared to filled bands. This follows because the energy of a state with two holes on Ni site $A$ and one on Ni site $B$ is degenerate with the state with one hole on Ni site $A$ and two on Ni site $B$ and

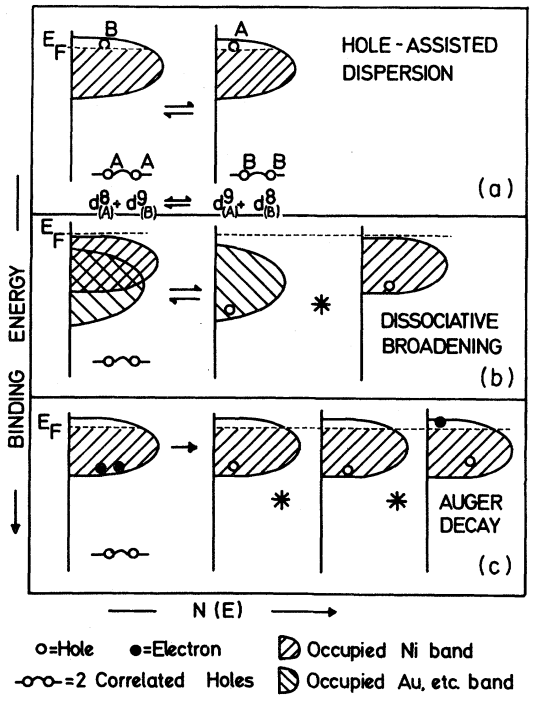


FIG. 13. Schematic illustration of the mechanisms of broadening of the Ni $L_3VV$ Auger spectra. (a) hole-assisted dispersion, (b) dissociational broadening due to decay into uncorrelated holes on different sites, and (c) Auger lifetime broadening.

these states mix via the one-hole hopping integral. We call this process *hole-assisted dispersion.* It is unlike the filled-band case where an energy transfer of $U$ is required for the pair to first separate. One could crudely estimate the upper limit of hole-assisted dispersion to be $W$ times the fraction of Ni atoms in a $d^9$ configuration if the hopping integrals are taken to be the same for Ni $d^9$-$d^{10}$ and $d^8$-$d^9$ hopping. As Ni itself has 9.4 electrons/atom in the $d$ band (0.6 holes) and $W \sim 4$ eV, the excess width calculated for this mechanism is of the order of 2.4 eV. This is probably an upper limit, but it is large and the effect can be isolated in our data, as discussed below. As explained in paper I it is difficult to estimate exactly the amount and distribution of Ni $d$ character in the unoccupied bands of Ni alloys. However, this mechanism is formally inoperative in alloys with no direct Ni-Ni interactions which will be useful in isolating the effect.

The second contribution to the excess width due to interaction between the two-hole band states and the bands of the partner element is illustrated in the middle panel of Fig. 13. In Sec. II we essentially considered broadening of the two-hole bound state arising from its mixing with delocalized band states. In the alloys we have the interesting possibility that the two-hole bound state may mix with states with one hole in the "Ni band" and one hole in the "partner-element bands". Qualitatively, the size of this *dissociational broadening* should be large if the Ni two-electron BE derived from Auger spectra is in a large-DOS region of "mixed convolution" of the nickel with the partner bands, i.e., if energy is conserved in the reaction

$$3d^8 \rightarrow 3d^9 + \text{hole in partner band}, \qquad (8)$$

then there will be a lifetime broadening from dissociation of the $3d^8$ virtual two-hole bound state. An example of this is the NiAu alloy. The effect should be small when the DOS of the mixed convolution is small at the $3d^8$ energy. This latter case applies to La-Ni alloys for instance where the La bands are only about 1.5-eV wide so that the bottom of the mixed convolution is above the $3d^8$ energy.

The third broadening process is a lifetime-broadening effect. The open $d$ bands, and consequent high DOS near the Fermi level enhance a decay mechanism involving the formation of electron-hole pairs from the two-hole state. We may argue that this mechanism is not too important because it involves interatomic Auger-type matrix elements. There are thus two processes that could significantly contribute to the excess Ni $L_3VV$ width and it is difficult to find systems in which the two contributions cannot be varied fully independently. We shall show that both contribute to the observed trends.

First of all we note that there are a few alloys in Table II with very large Ni $L_3VV$ widths, such a AuNi, CuNi, and PdNi (see also Fig. 11). In these cases, the partner DOS is exceptionally high, so the linewidth is certainly dominated by the contribution from dissociational broadening.

In order to discuss the hole-assisted dispersional broadening the number of nearest-neighbor nickel-pair interactions is listed in Table II. In every series with a given partner, the excess Auger width decreases with the Ni-Ni coordination number. This is certainly an indication that hole-assisted dispersion is operative here. Good examples are provided by La- and Ce-Ni alloys where the dissociational broadening is not operative (see below) and the excess widths are almost linearly dependent on coordination number.

To examine the effect of dissociational broadening, we first examine the alloys with no nearest-neighbor Ni-Ni contacts, where hole-assisted dispersion is not operative. Here the excess width is smallest for $La_7Ni_3$ and $Ce_7Ni_3$. The La and Ce bands extend only to 1.5–2 eV below $E_F$ (paper I) so that the combined BE at the bottom of the fold of Ni $d$ with the La-Ce bands is only approximately 5–5.5 eV below $E_F$ which is 1.5–2 eV above the Ni $d^8$ energy. The contribution to dissociational broadening is thus minimal.

Other measurements of the excess Ni $L_3VV$ width in alloys with no Ni-Ni contacts are 0.6 eV for $Th_7Ni_3$, 1.05 eV for $Al_3Ni$ (Table II), and $\sim 3$ eV for 2.5 at.% Ni in Au.[59] These results show a trend to increasing excess width with increasing density of two-hole states in the fold of the Ni and partner bands at the Ni $d^8$ energy. In the other alloys both mechanisms are usually operative, although dissociative broadening always plays a small role in Ni alloys with metals whose occupied bands are narrow, such as La and Ce.

Experiments that might strengthen these arguments are as follows:

(1) Ni $L_3VV$ measurements of other dilute Ni alloys where there are no nearest-neighbor nickel pairs.

(2) Co $L_3VV$ measurements on Co alloys where the number of $3d$ holes is larger than in Ni and larger contributions of hole-assisted dispersion may be observed.

(3) If the two-hole (virtual) bound state from the Auger process in an alloy should be accidentally degenerate with a shallow core hole, this might lead to unusual Auger line shapes.

## V. CONCLUDING REMARKS

The investigations reported here aimed to cover the range of variations in Ni $L_3VV$ spectra from in intermetallic compounds. In all cases the main $^1G$ final state of the Ni $L_3VV$ Auger peak had the same energy as the VB satellite (see paper I, Table VI) but the Auger spectra are more suitable for investigation of Coulomb interactions. The values of $U^A$ determined here were nearly constant for all the Ni alloys studied. This is attributed to "excitonic" screening involving Ni $s$ and $p$ orbitals and thus is unaffected by chemical effects on the initial-state Ni $d$-character distribution. The Ni Auger linewidths were shown to contain contributions of up to $\sim 3$ eV from new broadening mechanisms. These are hole-assisted dispersion of the localized $d^8$ final state in the Ni $L_3VV$ Auger spectra and dissociation broadening in which one hole from the $d^8$ configuration hops into the "partner band".

Inclusion of $d^8$-multiplet effects in the Cini formalism is important for explanation of the observed $L_3VV$ line shape. The results indicate that the $^3F$ $d^8$ states in Ni are similar in energy to bandlike Ni states, which is important for the understanding of magnetism in Ni. We believe some work is desirable to incorporate this fact in band-structure calculations of Ni, although we cannot at present suggest a theoretial scheme to do so.

We believe that the theoretical treatment outlined here could be applied to Auger spectra from Ni in other environments such as in compounds with nonmetals, or dilute alloys. In such studies it would be possible to vary the important parameters, such as the Ni $d$-band width and the number of Ni $d$ holes in a more extreme way. It would also be useful to study the $L_3VV$ Auger spectra of other transition-metal intermetallics, e.g., Co alloys where the hole concentration is larger, in a more systematic way.

## ACKNOWLEDGMENTS

We are grateful to Professor M. Campagna for his support and encouragement of this work and to J. Keppels and Ch. Freiburg for technical assistance. We also thank J. Fink, W. Gudat, R. O. Jones, D. Spanjaard, and G. Treglia for extensive discussions and comments on the manuscripts.

---

*Present address: Bell Telephone Labs, Murray Hill, New Jersey 07974.

[1]J. C. Fuggle, F. U. Hillebrecht, R. Zeller, Z. Zołnierek, P. Bennett, and Ch. Freiburg, this issue, Phys. Rev. B 27, 2145 (1983).

[2]F. U. Hillebrecht, J. C. Fuggle, P. Bennett, Z. Zołnierek, and Ch. Freiburg, preceding paper, Phys. Rev. B 27, 2179 (1983).

[3]E. Antonides, E. C. Janse, and G. A. Sawatzky, Phys. Rev. B 15, 1669 (1977).

[4]L. I. Yin, T. Tsang, and I. Adler, Phys. Rev. B 15, 2974 (1977).

[5]M. Cini, Solid State Commun. 24, 681 (1977); Phys. Rev. B 17, 2788 (1978).

[6]E. Antonides and G. A. Sawatzky, in *Proceedings of the International Conference on the Physics of Transition Metals, Toronto, 1977,* edited by M. J. G. Lee, J. M. Perz, and E. Fawcett (IOP, London, 1978), p. 134.

[7]G. A. Sawatzky, Phys. Rev. Lett. 39, 504 (1977).

[8]G. A. Sawatzky, and A. Lenselink, Phys. Rev. B 21, 1790 (1980).

[9]G. Tréglia, M. C. Desjonqueres, F. Ducastelle, and D. Spanjaard, J. Phys. C 14, 4347 (1981).

[10]T. Jach and C. J. Powell, Phys. Rev. Lett. 46, 953 (1981).

[11]P. T. Andrews, T. Collins, and P. Weightman, J. Phys. C 14, L957 (1981).

[12]J. C. Fuggle, P. A. Bennett, F. U. Hillebrecht, A. Lenselink, and G. A. Sawatzky (unpublished).

[13]P.J. Bassett, T. E. Gallon, J. A. D. Matthew, and M. Prutton, Surf. Sci. 35, 63 (1973); J. A. D. Matthew, J. Phys. C 11, L47 (1978).

[14]C. J. Powell, Phys. Rev. Lett. 30, 1179 (1973).

[15]E. D. Roberts, P. Weightman, and C. E. Johnson, J. Phys. C 8, L301 (1975); P. Weightman and P. T. Andrews, *ibid.* 12, 943 (1979).

[16]P. J. Feibelman, E. J. McGuire, and K. C. Pandey, Phys. Rev. B 15, 2202 (1977); 17, 690 (1978).

[17]D. J. Jennison, Phys. Rev. B 18, 6865 (1978); Phys. Rev. Lett. 40, 807 (1978).

[18]J. C. Fuggle, in *Electron Spectroscopy, Theory, Techniques and Applications IV,* edited by C. R. Brundle and A. D. Baker (Academic, London, 1981), p. 85.

[19]T. E. Gallon, in *Electron and Ion Spectroscopy of Solids,* edited by L. Fiermans, J. Vennik, and W. Dekeyser (Plenum, New York, 1978), p. 230.

[20]J. Hubbard, Proc. R. Soc. London 276, 238 (1963); 277, 237 (1964); 281, 401 (1964).

[21]C. Herring, in *Magnetism,* edited by G. T. Rado and H. Suhl (Academic, London, 1966), Vol. IV.
[22]D. M. Edwards, Physica 91B, 3 (1977).
[23]J. H. van Fleck, Rev. Mod. Phys. 25, 220 (1953).
[24]E. Antonides, Ph.D. thesis, University of Groningen, Holland, 1977 (unpublished).
[25]S. P. Kowalczyk, R. A. Pollak, F. R. McFeely, L. Ley, and D. A. Shirley, Phys. Rev. B 8, 2387 (1973).
[26]S. P. Kowalczyk, L. Ley, F. R. McFeely, R. A. Pollak, and D. A. Shirley, Phys. Rev. B 9, 381 (1974).
[27]J. C. Fuggle, E. Källne, L. M. Watson, and D. J. Fabian, Phys. Rev. B 16, 750 (1977).
[28]P. Weightman, J. F. McGilp, and C. E. Johnson, J. Phys. C 9, L585 (1976).
[29]M. Cini, Surf. Sci. 87, 483 (1979).
[30]C. E. Moore, *Atomic Energy Levels,* Natl. Bur. Stand. (U.S.) Circ. No. 467 (U.S. GPO, Washington D.C., 1957).
[31]S. Hüfner and G. K. Wertheim, Phys. Lett. 51A, 299, 301 (1975).
[32]P. C. Kemeny and N. J. Shevchik, Solid State Commun. 17, 255 (1975).
[33]C. Guillot, Y. Ballu, J. Paigné, J. Lecante, K. P. Jain, P. Thiry, R. Pinchaux, Y. Pétroff, and L. M. Falicov, Phys. Rev. Lett. 39, 1632 (1977).
[34]D. R. Penn, Phys. Rev. Lett. 40, 568 (1978); 42, 921 (1979).
[35]L. C. Davis and L. A. Feldkamp, J. Appl. Phys. 50, 1944 (1979); Solid State Commun. 34, 141 (1980); Phys. Rev. B 22, 3644 (1980).
[36]L. A. Feldkamp and L. C. Davis, Phys. Rev. Lett. 43, 151 (1979); 44, 673 (1980).
[37]A. Liebsch, Phys. Rev. Lett. 43, 1431 (1979); Phys. Rev. B 23, 5203 (1981).
[38]G. Treglia, F. Ducastelle, and D. Spanjaard, Phys. Rev. B 21, 3729 (1980); J. Phys. (Paris) 41, 281 (1980).
[39]N. Mårtenson and B. Johansson, Phys. Rev. Lett. 45, 482 (1980).
[40]J. C. Fuggle and Z. Zołnierek, Solid State Commun. 38, 799 (1981).
[41]We note that the result of Treglia *et al.* given in Fig. 4 has the same shape as that given in Ref. 9, but that Treglia *et al.* used a different way of aligning the spectra in that paper.
[42]D. R. Jennison, H. H. Madden, and D. M. Zehner, Phys. Rev. B 21, 430 (1980).
[43]J. F. McGilp and P. Weightman, J. Phys. C 11, 643 (1978).
[44]J. C. Slater, *Quantum Theory of Atomic Structure* (McGraw-Hill, New York, 1960). Vol. II, p. 294.
[45]E. J. McGuire, Phys. Rev. A 16, 2365 (1977); Sandia Laboratory Report No. Sc-RR-71 00 75 (unpublished).
[46]This has the result of broadening the line shape and simulating part of the experimental and core-level lifetime broadening and effects of dispersion of the two-hole state. It produces less numerical and computational problems than folding the Cini result with Lorentzian and Gaussian functions.
[47]J. B. Mann, Los Alamos Scientific Laboratory Report No. LASL-3690 (unpublished).
[48]A. C. Parry-Jones, P. Weightman, and P. T. Andrews, J. Phys. C 12, 1587,3635 (1979).
[49]P. Weightman and P. T. Andrews, J. Phys. C 13, 3295,L815,L821 (1980).
[50]S. Doniach and M. Šunjić, J. Phys. C 3, 285 (1970).
[51]P. Steiner, F. J. Reiter, H. Höchst, S. Hüfner, and J. C. Fuggle, Phys. Lett. 66A, 229 (1978).
[52]H. W. Haak, G. A. Sawatzky, and T. D. Thomas, Phys. Rev. Lett. 41, 1825 (1978).
[53]The difference between our value for $U^A(^1G)$ (3.65 eV) and that of Jach and Powell (Ref. 10) (2.5 eV) has two sources. Jach and Powell used a published value of 852.4 for the $L_3$ binding energy whereas we used 852.65 measured in our own instrument [see also J. C. Fuggle and N. Märtensson, J. Electron. Spectrosc. Relat. Phenom. 21, 275 (1980)]. Also Jach and Powell used the calculated band structure of Wang and Callaway [Phys. Rev. B 15, 298 (1977)] for the valence band where we used the XPS valence band without the satellite in order to facilitate comparison with the alloys.
[54]S. J. Oh, J. W. Allen, I. Lindau, and S. C. Mikkelsen Jr. (unpublished).
[55]L. Ley, S. P. Kowalczyk, F. R. McFeely, R. A. Pollak, and D. A. Shirley, Phys. Rev. B 8, 2392 (1973).
[56]R. Hoogewijs, L. Fiermans, and J. Vennik, Chem. Phys. Rev. 38, 471 (1978).
[57]M. Ohno, Phys. Scr. 21, 589 (1980).
[58]B. Johansson and N. Märtensson, Phys. Rev. B 21, 4427 (1980).
[59]A. Bosch, H. Feil, G. A. Sawatzky, and N. Märtensson, Solid State Commun. 41, 355 (1982).